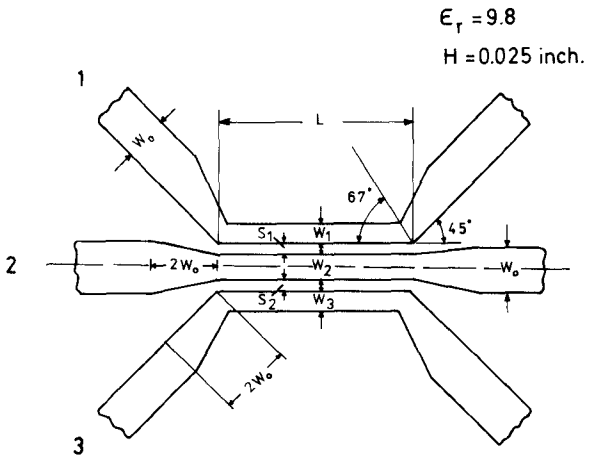

Geometric Dimensions	$W_{1,3}$ (μm)	W_2 (μm)	$S_{1,2}$ (μm)	L (mm)	W_o (μm)
Coupler of Ref [1]	431.8	431.8	190.5	7.690	600
Present Coupler	431.8	550.23	190.5	7.589	600

Fig. 12. Configuration and dimensions of the two couplers

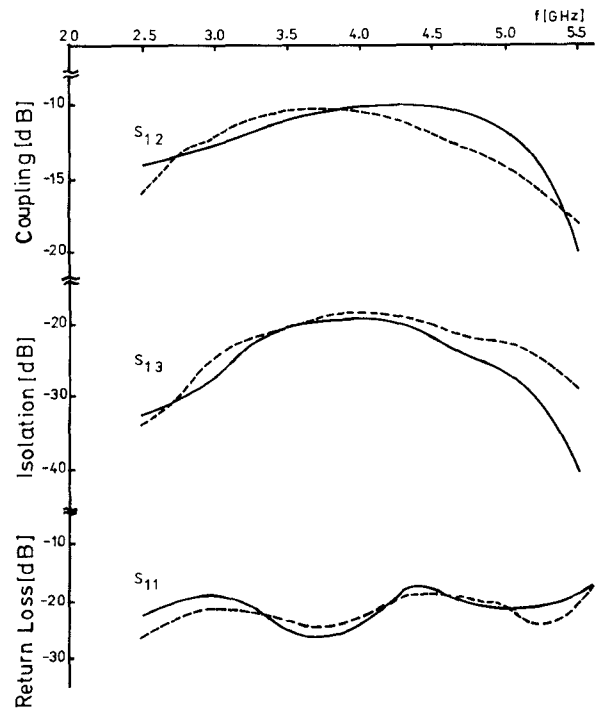

Fig. 13. Comparison of the behavior of the three-line coupler of this paper —— and that of [1]---.

on the present equal-impedance lines, showed that the latter gives, in general, a better behavior for the present example. In the present work, no attempt has been made to achieve a superior performance of the equal-impedance system over the equal-width system or vice versa.

Acknowledgment

The authors would like to thank the staff of the Microstrip Laboratory, Electronics Research Institute, National Research Centre, Cairo, Egypt, for the fabrication of the couplers, and the staff of the Microwave Laboratory, Military Technical College, Cairo, Egypt, for the measuring facilities.

References

[1] D. Pavalidis and H. L. Hartnagel, "The design and performance of three-line microstrip couplers," *IEEE Trans. Microwave Theory Tech.*, vol. MTT-24, pp. 631–640, Oct. 1976.

[2] V. Tulaja, B. Schiek, and J. Köhler, "An integrated 3-dB coupler with three strips," *IEEE Trans. Microwave Theory Tech.*, vol. MTT-26, pp. 643–645, Sept. 1978.

[3] R. J. Collier and N. A. El-Deeb, "Microstrip coupler suitable for use as a 6-port reflectometer," *Proc. Inst. Elec. Eng.*, vol. 127, pt. H, pp. 87–91, Apr 1980.

[4] L. Gruner, "Nonsymmetrical three-line microstrip couplers," in *Proc. Eur. Microwave Conf.*, A 10-3, 1981, pp. 844–849.

[5] R. J. Collier and N. A. El-Deeb, "On the use of a microstrip three-line system as a six-port reflectometer," *IEEE Trans. Microwave Theory Tech.*, vol MTT-27, pp. 847–853, Oct. 1979.

[6] V. K. Tripathi, Y. K. Chin, and H. Lee, "Interdigital multiple coupled microstrip dc blocks," in *Proc. Eur. Microwave Conf.*, A8-4, 1982, pp. 632–636.

[7] V. K. Tripathi, "On the analysis of symmetrical three-line microstrip circuits," *IEEE Trans. Microwave Theory Tech.*, vol. MTT-25, pp. 726–729, Sept. 1977.

[8] B. L. Lennartsson, "A network analogue method for computing the TEM characteristics of planar transmission lines," *IEEE Trans. Microwave Theory Tech.*, vol. MTT-20, pp. 586–591, Sept. 1972.

[9] F.- Y. Chang, "Transient analysis of lossless coupled transmission lines in a nonhomogeneous dielectric medium," *IEEE Trans. Microwave Theory Tech.*, vol. MTT-18, pp. 616–626, Sept. 1970.

[10] N. A El-Deeb, E. A. F. Abdallah, and M. B. Saleh, "Design parameters of inhomogeneous asymmetrical coupled transmission lines," *IEEE Trans. Microwave Theory Tech.*, vol. MTT-31, pp. 592–596, July 1983.

[11] L. S Napoli and J. J. Hughes, "Characteristics of coupled microstrip lines," *RCA Rev.*, pp. 479–498, Sept 1970.

Broad-Band Permittivity Measurements Using the Semi-Automatic Network Analyzer

JOHN NESS

Abstract—**This paper outlines the use of the network analyzer to measure the dielectric properties of materials over a broad frequency range. The method described here is based on transmission techniques with simple procedures for obtaining initial estimates and unambiguous solutions for the dielectric parameters. A further feature is that this measurement technique provides a degree of self-checking for inconsistent results.**

I. Introduction

The semiautomatic network analyzer (SANA) is a powerful tool for the measurement of the permittivity of materials. Most of the classical techniques [1] for permittivity measurements can be adapted for the SANA, and with the latest generation of equipment, very broad-band measurements can be done very efficiently. The technique described here is based on transmission measurements, and can be applied to fully or partially filled guide, although the latter method is more complex.

II. Measurement Theory

With suitable calibration standards and procedures, the SANA can be used to measure samples mounted in coaxial line, waveguide, or stripline-type structures. In general, the coaxial and waveguide methods will provide the best accuracy since precision calibration standards are available for these systems. The coaxial line provides the maximum measurement bandwidth, but sample mounting is often difficult with this technique.

Manuscript received October 9, 1984; revised June 5, 1985.

The author is with the Microwave Technology Development Centre, Electrical Engineering Department, University of Queensland, Brisbane, Australia 4067

0018-9480/85/1100-1222$01.00 ©1985 IEEE

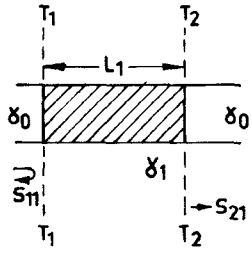

Fig. 1. Loaded section of guide.

For a guide fully filled with nonmagnetic material, the complex permittivity can, in theory, be obtained from a measurement of either the reflection or transmission coefficient. Although the reflection technique seems to be the most commonly used, the transmission technique has several advantages when using the SANA. The transmission measurement offers a wide dynamic range, and the problems of achieving accurate measurements of both high- and low-reflection coefficients with standard calibration techniques are avoided [2]. Furthermore, the transmission measurements provide good initial estimates of the dielectric constant and, if necessary, the loss factor which lead to easy solutions for the transcendental equations.

Consider the loaded guide configurations shown in Fig. 1. The reflection and transmission coefficients at the reference planes T_1 and T_2 are given by the well-known equations [3]

$$S_{11} = \frac{(\gamma_1 - \gamma_0)^2(e^{-\gamma L_1} - e^{\gamma L_1})}{(\gamma_1 + \gamma_0)^2 e^{\gamma L_1} - (\gamma_1 - \gamma_0)^2 e^{-\gamma L_1}} \tag{1}$$

$$S_{21} = \frac{4\gamma_1\gamma_0}{(\gamma_1 + \gamma_0)^2 e^{\gamma L_1} - (\gamma_1 - \gamma_0)^2 e^{-\gamma L_1}} \tag{2}$$

where

$$\gamma_0 = \alpha_0 + j\beta_0 \qquad (\alpha_0 \simeq 0)$$
$$\gamma_1 = \alpha_1 + j\beta_1.$$

In general, the input and output sections are air-filled but sometimes low-loss foam is placed in these sections for measurements on powders or viscous liquids. The propagation coefficient γ_1 is related to the dielectric constant and loss tangent of the material by the following equations [4]:

$$\epsilon_r = \frac{\lambda_0^2}{4\pi^2}(\beta_1^2 - \alpha_1^2) \quad \beta_0 = \frac{2\pi}{\lambda_0} \quad \tan\delta = \frac{2\alpha_1\beta_1}{\beta_1^2 - \alpha_1^2} \tag{3}$$

for the coaxial line and

$$\epsilon_r = \frac{\dfrac{1}{\lambda_c^2} + \dfrac{\beta^2 - \alpha^2}{4\pi^2}}{\dfrac{1}{\lambda_c^2} + \dfrac{1}{\lambda_0^2}}, \qquad \beta_0 = \left[\omega^2\mu_0\epsilon_0 - \left(\frac{2\pi}{\lambda_c}\right)^2\right]^{1/2}$$

$$\tan\delta = \frac{2\alpha\beta_1}{\beta_1^2 - \alpha_1^2 + \dfrac{4\pi^2}{\lambda_c^2}} \tag{4}$$

where λ_c is the cutoff wavelength of waveguide ($\lambda_c = 2a$ for rectangular waveguide) and λ_0 is the free-space wavelength.

Having measured S_{11} or S_{21} and γ_0 is known, then the solution of (1) or (2) yields γ_1 from which ϵ_r and $\tan\delta$ can be calculated. In practice, the situation is not quite as straightforward, partly because of the multiplicity of solutions of (1) or (2). If a good initial estimate for ϵ_r is available, then the solution method is simplified. For the transmission techniques, very good estimates for ϵ_r are possible even for high-loss samples from the following approximations derived from the previous equations:

$$\epsilon_r \doteq \left(\frac{n150}{LF}\right)^2 \qquad \text{for coaxial line} \tag{5}$$

$$\epsilon_r \doteq \frac{\left(\dfrac{an}{L}\right)^2 + 1}{\left(\dfrac{aF}{150}\right)^2} \qquad \text{for rectangular waveguide} \tag{6}$$

where a (the waveguide width) and L (the sample length) are in millimeters, and F (the frequency) is in gigahertz. F is the frequency at which $\angle S_{21} = 0$ or 180°, n is even (2,4,6, etc.) for $\angle S_{21} = 0$ and odd (1,3,5, $\cdots$) for $\angle S_{21} = 180°$.

The value of the integer n is still not known but is easily found if the frequency range is sufficient to provide two or more frequency values where $\angle S_{21} = 0$ or 180°. For low-loss samples, the maximum values of $|S_{21}|$ correlate with $\angle S_{21} = 0$, 180° and the minimum values with $\angle S_{21} = 90$, 270°. For high-loss samples, maximum and minimum values of $|S_{21}|$ are not apparent but these points are easily identified from the phase reading. It is usually not necessary to start with an accurate estimate for $\tan\delta$. However, $\tan\delta$ can be estimated from the following formula if the frequencies F_1 and F_2 at successive $\angle S_{21} = 0$ and 180° phase points are found:

$$\tan\delta = \frac{95.5\ln(|S_{21}(F_1)|/|S_{21}(F_2)|)}{L(F_2 - F_1)\sqrt{\epsilon_r}}. \tag{7}$$

This equation was derived for the coaxial line but is a sufficiently good approximation for waveguide. With these initial estimates for ϵ_r and $\tan\delta$, the following formulas can be used to obtain α_1 and β_1 and so to calculate S_{21}:

$$\alpha_1 = \frac{2\pi}{\lambda_0}\left[\tfrac{1}{2}\epsilon_r\left\{(1+\tan^2\delta)^{1/2} - 1\right\}\right]$$

$$\beta_1 = \frac{2\pi}{\lambda_0}\left[\tfrac{1}{2}\epsilon_r\left(1 + (1+\tan^2\delta)^{1/2}\right)\right]^{1/2} \tag{8}$$

for the coaxial line and

$$\alpha_1 = \frac{2\pi^2}{\beta_1}\epsilon_r\frac{\tan\delta}{\lambda_0^2}$$

$$\beta_1 = \frac{1}{2}\left\{\frac{4\pi^2\epsilon_r}{\lambda_0^2} - \frac{4\pi^2}{\lambda_c^2} + 4\pi^2\left[\left(\frac{1}{\lambda_c^2} - \frac{\epsilon_r}{\lambda_0^2}\right)^2 + \epsilon_r^2\frac{\tan^2\delta}{\lambda_0^4}\right]^{1/2}\right\} \tag{9}$$

for waveguide.

The initial value for S_{21} is compared with the measured value, and by a series of successive iterations, the values of ϵ_r and $\tan\delta$ are incremented until the calculated value of S_{21} agrees with the measured value of S_{21} within experimental error. The convergence is very rapid even on the small computers typically used to control SANA's. The method used here first iterates ϵ_r until the calculated phase of S_{21} agrees with the measured value and then iterates $\tan\delta$ until the calculated and measured magnitude values of S_{21} are equal. Typically, only one additional cycle of this process is necessary to get simultaneous agreement of both magnitude and phase values.

III. Measurement Technique

The technique uses standard calibration and measurement procedures. That is, the system calibration is carried out with a short circuit, offset short circuit (waveguide) or open circuit (coaxial

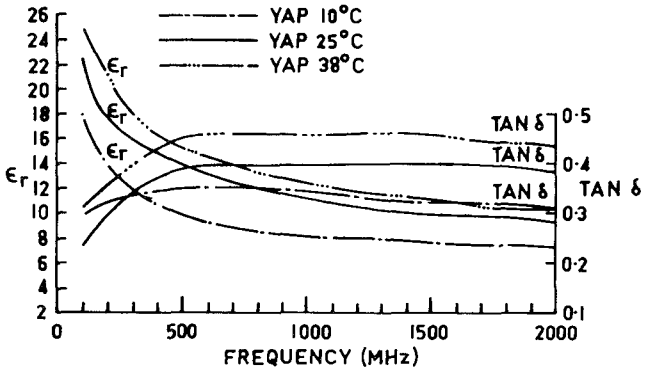

Fig. 2. Relative permittivity of honey as a function of frequency.

line), a matched or sliding load, and the through connection. With sexless connectors such as waveguide flanges, APC-7, and GR-900 coaxial connectors, symmetry of the mounting section for the sample is possible. For sexed connectors such as APC-3.5, one end of the coaxial section containing the sample should mate with a male connector and the other with a female connector. In this case for sexed, as well as sexless connectors, the calibration can be done at the input and output planes of the loaded guide section so that S_{21} and S_{11} are measured directly with no deembedding required.

Since the measurements are taken at discrete frequency points, it is unlikely that the frequencies at which $\angle S_{21} = 0$ or 180° will coincide with the measurement frequencies. However, simple linear interpolation will provide a close enough approximation. The estimates for ϵ_r and $\tan\delta$ are then entered into the computer for one frequency point and the iteration carried out to get the actual values. These values are then used as the initial estimate for the next frequency and so on. The convergence is quite rapid once the first values of ϵ_r and $\tan\delta$ are found. The program also prints out the return loss values as calculated from the values of ϵ_r and $\tan\delta$ and these should coincide with the measured values. If the wrong value of n has been selected, solutions of ϵ_r and $\tan\delta$ will usually be found but the return loss values will not coincide and ϵ_r and $\tan\delta$ will show a fast variation with frequency.

IV. Results

The above technique has been used to measure the dielectric properties of a range of materials over a broad frequency range. Fig. 2 shows the dielectric properties of some honey samples measured in a 14-mm coaxial line with low-loss foam dielectric used to contain the honey. The results were corrected to account for this foam. Fig. 3 shows similar results for coal samples measured in a range of rectangular waveguides. For the low moisture content samples, the dielectric properties vary quite slowly with frequency, whereas for the higher moisture content samples, $\tan\delta$ in particular increases fairly rapidly with frequency. The spread in the measured values is quite small, being about 2 percent for ϵ_r and 5 percent for $\tan\delta$. In this case, of course, it is the frequency-dependent properties of water which mainly determine the behavior of the dielectric properties. Although the use of the waveguide restricts the frequency range, it is much easier to pack coarse materials such as coal in rectangular waveguide rather than coaxial line. Table I shows typical data and compares the measured reflection coefficient for two coal samples with that calculated from the dielectric values obtained from the transmission coefficient. For the dry sample, the attenuation was

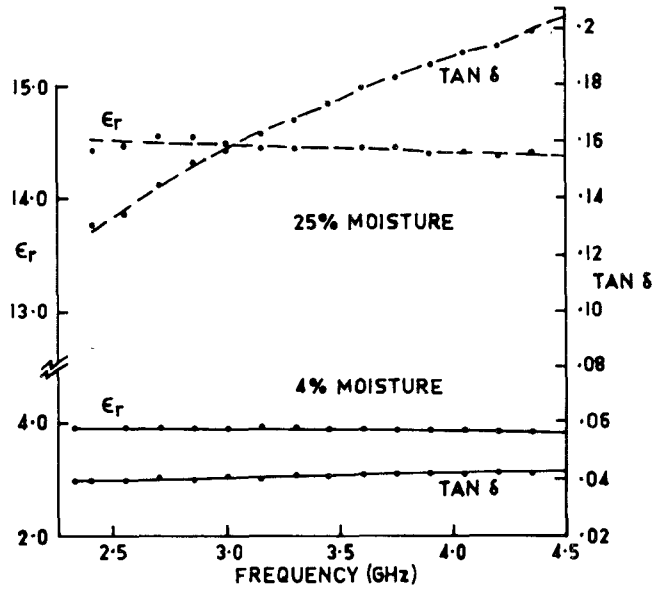

Fig. 3. Relative permittivity of coal as a function of frequency.

TABLE I
Typical Results for Dry and Moist (20 percent by Weight) Coal Samples in Rectangular Waveguide.

FREQ (GHz)	S_{21} dB	S_{21} deg	S_{11} (measured) dB	S_{11} (measured) deg	ϵ_r	Tan δ	S_{11} (calculated) dB	S_{11} (calculated) deg
2.4	4 84	-45	6.54	-167	2.494	.0378	6.89	-159.2
2.6	4.47	-131	8.14	156	2.518	.0371	7.69	156.5
2.8	3.96	137	9.36	-156	2.508	.033	8.97	-156 5
3.0	4.37	59	8.3	162	2.500	.0342	8.19	160.5
3.2	4.46	-29	11.94	-157	2.500	.0373	11.88	-159.4
3.4	4.47	-110	9.03	172	2.503	.0334	8.41	166.8
2.4	18.73	-138	3.29	173	9.886	.128	3.08	177.1
2.6	19.71	104	3.93	-180	9.972	.135	3.42	178.7
2.8	20.35	-5	4 03	-178	9.957	.138	4.08	178.2
3.0	22.39	-107	3.68	-180	9.875	.149	4.18	177.4
3.2	24.48	143	4.16	180	9.878	.158	4.46	177.8
3.4	25.29	37	4.22	179	9.856	.157	4.64	177.2
3.6	26.73	-62	4.34	177	9.766	.160	4.77	177.4

only about 5 dB and the reflection coefficient exhibits oscillatory behavior with frequency. For the 20-percent moisture content sample, the much higher attenuation means that the reflection coefficient is virtually that of an infinite length sample. Note that in this case the reflection coefficient is quite insensitive to frequency unlike the transmission coefficient. The errors, although not large, are significant and are due to several factors. One is the system calibration errors that occur when measuring high-reflection coefficients if a short and offset short circuit only are used in the calibration (instead of several offset short circuits). The other relates to the coal–air interface. With this powder material, it is difficult to maintain a flat, smooth surface across the waveguide. To check the validity of the technique, a 10-mm

length of pure water at 25°C was measured at 100-MHz increments from 8 to 12.4 GHz. The values of ϵ_r decreased from 67.2 to 59.5 and $\tan\delta$ increased from 0.371 to 0.557 over this frequency range. These results agree well with published data [5] and even for this high-loss and high-dielectric constant, the initial estimate given by (6) was within a few percent of the final result. No moding problems were evident during the measurements. The use of the measured values of the reflection coefficient to determine the dielectric properties resulted in a much larger spread in the values compared to the transmission method.

V. Partially-Filled Guides

It is not always possible to obtain or machine samples to completely fill a coaxial or rectangular waveguide section. In this case, (1) and (2) are no longer applicable. There are various ways to overcome this problem. Perhaps the most direct method of obtaining the propagation coefficient from the measurements is to measure the scattering parameters on two or three samples, identical except for length. If only two sample lengths are available, the propagation coefficient can be calculated directly from the measured values of S_{11} and S_{21} [6]. That is

$$\gamma = \frac{\ln\left[\left(\frac{S_{11}(2)-A}{S_{11}(1)-A}\right)\frac{S_{21}(1)}{S_{21}(2)}\right]}{L_1 - L_1} \tag{10}$$

$$A = \frac{B \pm C}{D} \qquad (|A| \leqslant 1)$$

$$B = S_{11}^2(1) - S_{11}^2(2) - S_{21}(1) + S_{21}^2(2)$$

$$C = \Big[\big(S_{11}^2(1) - S_{11}^2(2) - S_{21}^2(1) - S_{21}(2)\big)^2 - 4\big(S_{11}(1) - S_{11}(2)\big)\big(S_{11}(1)\big(S_{21}^2(2) - S_{11}^2(2)\big) - S_{11}(2)\big(S_{21}^2(1) - S_{11}^2(1)\big)\big)\Big]^{1/2}$$

$$D = 2\big(S_{11}(1) - S_{11}(2)\big).$$

Since the SANA measures both S_{11} and S_{21}, the procedure is quite efficient. In general, for partially-filled guides, the magnitude of S_{11} will be considerably less than one so the accuracy will be good.

Alternatively, if measurements are carried out on three samples of lengths, L_1, $L_1 + \Delta$, and $L_1 + 2\Delta$, then the propagation coefficient can be found from transmission measurements only [7]. That is

$$\gamma = \frac{1}{\Delta}\cosh^{-1}\frac{1}{2}\left[\frac{S_{21}(2)}{S_{21}(3)} + \frac{S_{21}(2)}{S_{21}(1)}\right]. \tag{11}$$

In the above equations, $S_{11}(i)$ and $S_{21}(i)$ are the measured values of reflection and transmission coefficients for sample L_i.

Equations (10) and (11) can also be used for fully-filled guides but are valid in the more general case where Z (the guide impedance) and γ are not explicitly related provided a single mode only is propagating. While (11) provides a simple explicit formula for γ, at certain frequencies and for particular lengths, γ is a very sensitive function of S_{21}. If measurements are taken at a number of frequencies, these points of high sensitivity may give spurious results which are easily identified, but if only one or two frequency points are used, then $S_{21}(i)$ must be measured very accurately for reliable results.

With partially-filled guides, the problem still remains of relating the propagation coefficient γ to the material properties. Exact methods [8] are available for full-height samples across either waveguide dimension or in coaxial line. However, for partial-height samples, perturbation on approximation methods must be used.

VI. Discussion

Provided the conventional caveats concerning guide loss, sample fit, and orientation, etc., are observed, then the accuracy of these techniques depend on the accuracy of the SANA, the repeatability of the connectors, and the electrical length of the sample. Since the techniques described are for broad-band measurements, it is not practical to select sample lengths to give the optimum accuracy as is commonly done for single-frequency measurements. It is, of course, necessary to select sample lengths so that the minimum value of S_{21} will be well within the dynamic range of the SANA. The new generation of network analyzers (e.g., HP 8510T) with precision standards will give highly accurate results over very wide frequency ranges. The measurements described here were done using an HP 8409A network analyzer and so maximum accuracy is not expected. It is difficult to give specific figures for accuracy but, in general, measurement repeatability was typically within ± 0.15 dB and $\pm 2.5°$ for the samples measured. The effect of these errors will depend on the loss and line length of the sample being measured. For relatively short or low-loss samples, significant errors in ϵ_r and $\tan\delta$ may occur; but since multiple values are measured, spurious values are easily identified or can be averaged out. In most cases, however, the errors in ϵ_r and $\tan\delta$ arising from the measurement system inaccuracies are less than a few percent.

Similar equations and procedures can be developed for the reflection measurements with either a matched or short-circuited termination. The transmission technique does offer several advantages, particularly for relatively high-loss heterogeneous materials such as moist coal and other powder material. The transmission technique tends to "average out" longitudinal variations that may occur in such samples. Moreover, for high-loss samples, the reflection coefficient is relatively insensitive to dielectric properties. At 10 GHz, for example, a change in ϵ_r from 4.0 to 4.1 for a 50-mm-long high-loss ($\tan\delta = 0.1$) sample in X-band waveguide results in only a 3° change in the phase of the reflection coefficient but a 16° change in the transmission phase. In general, then, the transmission technique provides a simple accurate method for determining the dielectric properties over a wide range and for a diversity of material types. The only adaption to the standard technique is to vary the length of the sample when necessary so that the dynamic range of the SANA is not exceeded. Since the dynamic range is as high as 60 dB, only a small number of lengths are necessary to cover an enormous range of materials.

Acknowledgment

The author wishes to thank R. Young and P. Bradley of MITEC for assistance with the measurements and computer programs, and N. Cutmore of CSIRO, Lucas Heights, Sydney, for provision of all the coal samples.

References

[1] M. Sucher and J. Fox, *Handbook of Microwave Measurements*, vol. II. New York: Polytechnic Press, Wiley, 1963, ch. 9.

[2] G. R Cobb, J. Fitzpatrick, and J. Williams, "ANA techniques differ," *Microwave Syst. News*, vol. II, no. 11, pp. 27–35, Nov. 1981.

[3] A. Datta and B Nag, "Techniques for the measurement of complex microwave conductivity and the associated errors." *IEEE Trans. Microwave Theory Tech*., vol 18, pp. 162–170, Mar. 1970.

[4] A Von Hippel, *Dielectric Materials and Applications* New York: Wiley, 1954, ch. 2.
[5] S S. Stuchly and M Hamid, "Physical parameters in microwave heating processes," *J. Microwave Power*, vol. 7, no. 2, figs. 5 and 6, p 124, 1972.
[6] F. Gardiol and O. Parriaux, "Excess losses in *H*-plane loaded waveguide," *IEEE Trans Microwave Theory Tech.*, vol. 21, pp. 457–461, July 1973.
[7] J. Ness, "Broadband permittivity measurements at microwave frequency," *IREE Dig. (Australia)*, pp 330–332, Sept. 1983.
[8] R. E. Collin, *Field Theory of Guided Wave*. New York: Mc Graw Hill, 1960.

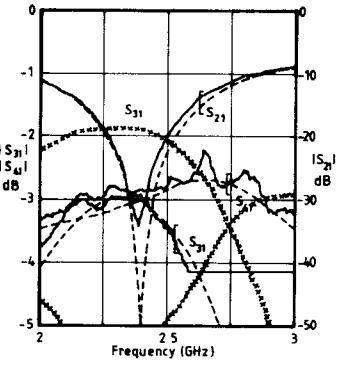

Fig. 1. Measured (solid line) and predicted (dotted line) response of uncompensated coupler.

Design Curves for −3-dB Branchline Couplers

A. F. CELLIERS AND
J. A. G. MALHERBE, SENIOR MEMBER, IEEE

***Abstract*—Design curves for −3-dB branchline couplers that include compensation for the junction discontinuities are presented. The curves are obtained by including an accurate model of a stripline *T*-junction in an optimization program.**

I. Introduction

The performance of −3-dB branchline couplers can be severely degraded by junction effects due to finite line widths. With increasing frequency, line widths become larger relative to line lengths and the junction effects become progressively more severe. The junction effects have been described by several authors [1]–[5]. Dydyk [6] compensates for the effects of the junctions by modifying the line lengths and both impedance levels of a branchline coupler; Cuhaci and Lo [7] compensate for these effects by the introduction of compensating stubs and impedance level changes. Chadha and Gupta compensate for discontinuities by cutting a small notch in the line [8].

An accurate equivalent circuit for the junction was obtained by comparing the predictions from [1]–[6] with a constructed coupler, and the junction properties thus obtained were used in an equivalent circuit of the branchline coupler. For each frequency of interest, and for a number of typical substrates for stripline realization, a computer optimization program was run to compute new branchline lengths and impedance levels that, together with the junction effect, will yield the correct amount of coupling at the desired center frequency.

II. Equivalent Circuit

A test coupler was fabricated at 2.5 GHz on 1/8-in GPS Polyguide and the coupler properties measured. This was compared to predictions based on the junction equivalents of [1]–[6], and it was found that, in most cases, strong deviation from the measured responses occurred. As an example, the prediction based on the model of [3] is shown in Fig. 1.

Fig. 1 also shows the measured response of the coupler, as well as the theoretical prediction, obtained with a modified version of

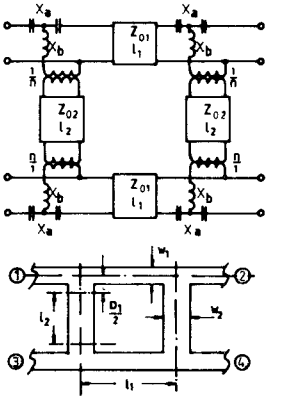

Fig. 2. Equivalent circuit of coupler including junction discontinuities.

the equivalent circuit described in [5], obtained by rearranging the equations. Referring to Fig. 2

$$n = \frac{n' \cos\left(\frac{2\pi}{\lambda_g} \cdot d'_{[WGH]}\right)}{\cos\left(\frac{2\pi d}{\lambda g}\right)} \tag{1}$$

$$\tan\left(\frac{2\pi}{\lambda g} d'_{[WGH]}\right) = \frac{Z_{01}}{Z_{02}} (n')^2 \frac{X_b}{Z_{01}} \tag{2}$$

$$\tan\left(\frac{2\pi d}{\lambda_g}\right) = \frac{-X_a}{Z_{01}} \tag{3}$$

$$n' = \frac{\sin(\pi D_2/\lambda_g)}{\pi D_2/\lambda_g} \tag{4}$$

$$n_1 = n'\sqrt{Z_{01}/Z_{02}} \tag{5}$$

$$\frac{X_a}{Z_{01}} = \frac{-D_2}{\lambda_g}[0.785 n_1]^2 \tag{6}$$

where $d'_{[WGH]}$ is obtained from [9]. The parameter d is calculated from (3), and defined in Fig. 2.

From [2], calculate

$$D_t = \begin{cases} w_t + \dfrac{2b\ln 2}{\pi} + \dfrac{t}{\pi}\left[1 - \ln\left(\dfrac{2t}{b}\right)\right], & \text{for } \left(\dfrac{w_t}{b}\right) > 0.5 \\ b\dfrac{K(k)}{K(k')} + \dfrac{t}{\pi}\left[1 - \ln\left(\dfrac{2t}{b}\right)\right], & \text{otherwise} \end{cases} \tag{7}$$

Manuscript received November 14, 1984; revised May 6, 1985. This paper is based on a dissertation by A F. Celliers submitted to the Department of Electrical and Electronic Engineering, University of Stellenbosch, South Africa, in partial fulfillment of the requirements of the M. Eng. degree.

A. F. Celliers is with the National Institute for Aeronautics and Systems Technology, Council for Scientific and Industrial Research, Pretoria, South Africa.
J. A. G. Malherbe is with the Department of Electronic Engineering and Laboratory for Advanced Engineering, University of Pretoria, South Africa

0018-9480/85/1100-1226$01.00 ©1985 IEEE